Journal Pre-proof

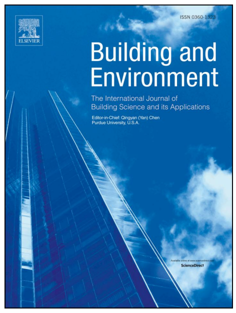

Operational carbon transition in the megalopolises' commercial buildings

Minda Ma, Wei Feng, Jingwen Huo, Xiwang Xiang

PII: S0360-1323(22)00935-0

DOI: https://doi.org/10.1016/j.buildenv.2022.109705

Reference: BAE 109705

To appear in: *Building and Environment*

Received Date: 16 August 2022

Revised Date: 23 September 2022

Accepted Date: 11 October 2022

Please cite this article as: Ma M, Feng W, Huo J, Xiang X, Operational carbon transition in the megalopolises' commercial buildings, *Building and Environment* (2022), doi: https://doi.org/10.1016/j.buildenv.2022.109705.

Graphical abstract

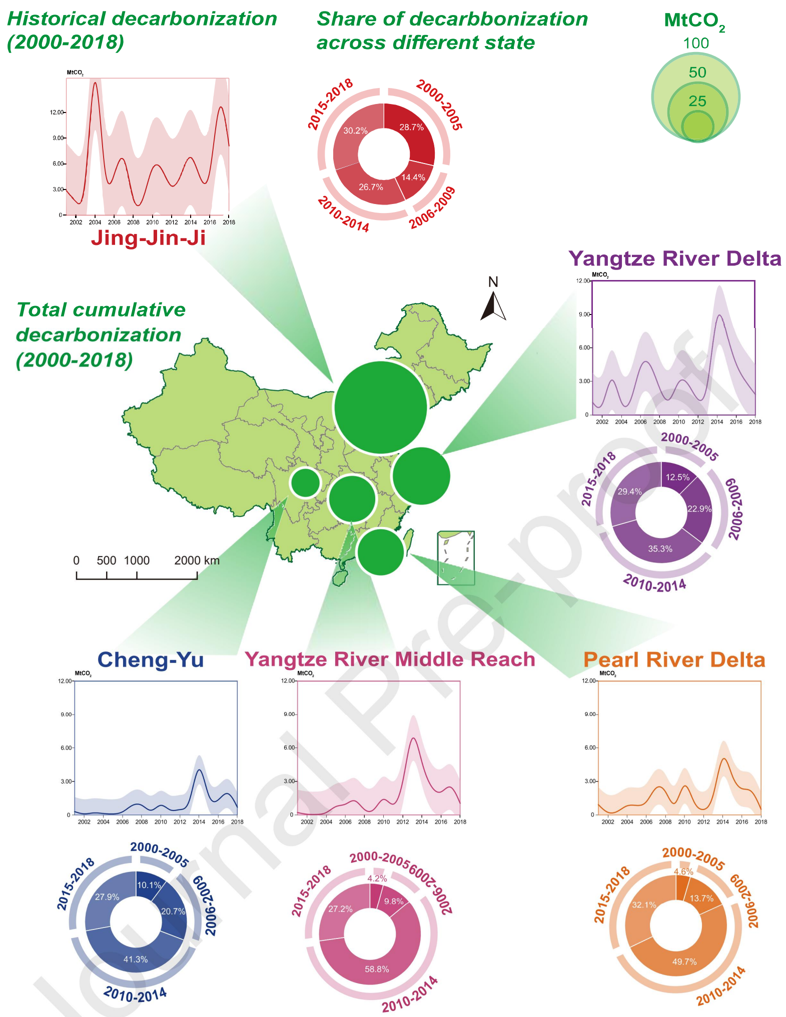

Graphical abstract. Operational decarbonization change of commercial buildings in megalopolises and the share of decarbonization at different stages (2000-2018). Note: the bubbles on the map indicate total cumulative decarbonization from 2000 to 2018, and the error bands in the line graph indicate one standard deviation.

Operational carbon transition in the megalopolises' commercial buildings

Minda Ma [1,], Wei Feng [2], Jingwen Huo [1], Xiwang Xiang [3 *]

1. Department of Earth System Science, Tsinghua University, Beijing 100084, PR China
2. Building Technology & Urban Systems Division, Lawrence Berkeley National Laboratory, Berkeley, CA 94720, USA
3. School of Management Science and Real Estate, Chongqing University, Chongqing 400045, PR China

- First author: **Dr. Minda Ma**, Email: maminda2020@tsinghua.org.cn
  maminda@tsinghua.edu.cn
- Corresponding author: **Dr. Xiwang Xiang**, Email: xiangxiwang@cqu.edu.cn

Graphical abstract

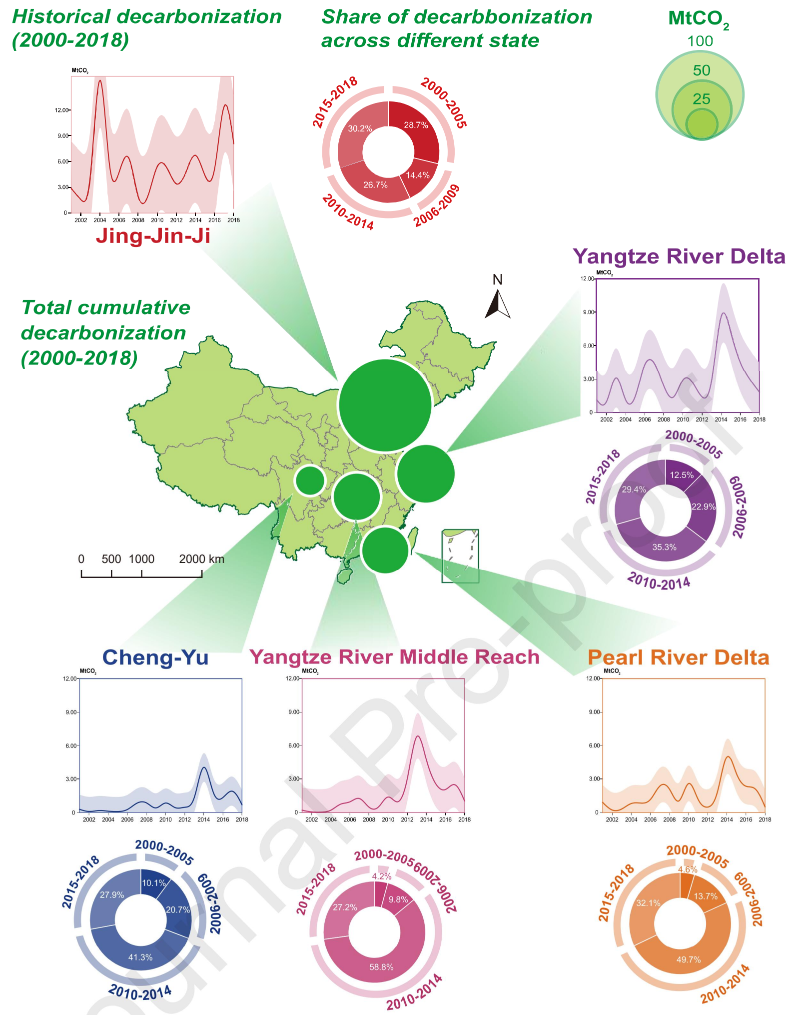

Graphical abstract. Operational decarbonization change of commercial buildings in megalopolises and the share of decarbonization at different stages (2000-2018). Note: the bubbles on the map indicate total cumulative decarbonization from 2000 to 2018, and the error bands in the line graph indicate one standard deviation.

Highlights

- GDIM was used to investigate drivers, decoupling, and mitigation of operational carbon changes.
- The effects of economic development and energy use are key to increasing operational carbon.
- Operational carbon emissions decoupled from economic effects in most megalopolises since 2009.
- Decarbonization level in five megalopolises was 233.1 Mt, with a decarbonization efficiency of 4.4%.
- Deep decarbonization strategies for commercial building operations in megalopolises were reviewed.

Abstract

Megalopolises are important political and economic centers and offer the best opportunities for decarbonizing commercial building operations. This study estimates the decarbonization level of commercial buildings from China's five major megalopolises (Jing-Jin-Ji, Yangtze River Delta, Pearl River Delta, Yangtze River Middle Reach, and Cheng-Yu) through the generalized Divisia index method, considering the impacts of socio-economy, technology evolution, and climate. Results found the following: First, economic growth effects [service industry added value (42.2%) and gross domestic product (36.5%)] and energy consumption (23.8%) were the main drivers of the spike in operational carbon emissions of the megalopolises from 2000–2018. Second, except for Cheng-Yu, operational carbon emissions were decoupled from economic growth effects since 2009, with the most significant decoupling status occurring in Jing-Jin-Ji, and technical effects being the main factor leading to the decoupling. Third, the five megalopolises cumulatively decarbonized 233.1 mega-tons of carbon dioxide ($MtCO_2$), offsetting 4.4% of the operational carbon of commercial buildings, with the highest decarbonization level in Jing-Jin-Ji (5.7 $MtCO_2$ per yr, 7.8 kilograms of carbon dioxide per square meter per yr, and 55.6 kilograms of carbon dioxide per capita per yr). Furthermore, current decarbonization strategies for megalopolises are reviewed to plan for future low-carbon developments. Overall, this study assesses the operational decarbonization change of commercial buildings in Chinese megalopolises. The findings help inform building of sector pathways toward China's carbon peaking and neutral goals and develop global low-carbon cities.

Keywords

Megalopolises;

Operational carbon emissions;

Commercial buildings decarbonization;

Carbon neutrality goal;

Generalized Divisia index method.

Abbreviation notation

GDIM –Generalized Divisia Index Method

GDP – Gross Domestic Product

IBED – International Building Emission Dataset

IDA – Index decomposition analysis

LMDI – Log-Mean Divisia Index

Nomenclature

C – Carbon emissions

E – Energy consumption

F – Gross floor space

G – Gross Domestic Product

G_s – Gross Domestic Product of service industry

Gtoe – Giga-ton of standard oil equivalent

$GtCO_2$ – Giga-ton of carbon dioxide

$kgCO_2$ – Kilograms of carbon dioxide

$MtCO_2$ – Megatons of carbon dioxide

P – Population

φ – Decarbonization effort index

ΔC – Change in operational carbon emissions

ΔD – Decarbonization effort

ΔDC – Total decarbonization

ΔDF – Decarbonization per floor space

ΔDP – Decarbonization per capita

1. Introduction

Buildings, the largest energy-consuming and emitting sector in China, are the last mile toward the carbon neutral century [1]. The latest evidence shows that China's building sector consumed 1.6 giga-ton of standard oil equivalent (Gtoe) and emitted nearly five giga-ton of carbon dioxide ($GtCO_2$) in 2019, which accounts for 50.0% of the anthropogenic emissions [2]. Meanwhile, the service industry's rapid urbanization and economic growth have led to a surge in commercial building (see the definition in Appendix A) energy demand, resulting in a 3.7-fold increase in operational carbon emissions over almost two decades [3]. Notably, an increasing number of studies have confirmed that the decarbonization potential of commercial buildings exceeds the previously believed values [4, 5]. Hence, net-zero emissions from the building sector are significant to China's carbon peaking and neutral actions, with the decarbonization of commercial building operations playing a crucial role.

Megalopolises are the most densely populated areas for economic development [6] and core contributors to building energy consumption and emissions (especially for commercial buildings) [7]. For example, the Yangtze River Delta produced 19.8% of China's total GDP with 11.0% of the population on 2.2% of the land area in 2018 [8], and released nearly 12.4% of operational carbon emissions from China's commercial buildings [9]. Moreover, since megalopolises are usually located in the same climate zones and share similar building energy structures [10, 11]; they are often regarded as the best units for energy and climate policy implementation [12]. Currently, most countries have wisely tilted policies toward megalopolises [13]. For China, deep decarbonization of the operational carbon emissions of megalopolises is a necessary way of achieving low-carbon development of the building sector and a step toward achieving carbon peaking and neutral goals. **Nevertheless,** few studies have assessed the operational decarbonization levels of commercial buildings, especially among megalopolises in China. Therefore, three questions have been raised regarding commercial buildings in China's megalopolises.

- What drives the decarbonization of commercial buildings in China's megalopolises?
- How has the decoupling state of carbon emissions from economic growth changed?
- What is the level of decarbonization of commercial buildings, and how can it be facilitated?

To answer the above questions, this study estimates the historical decarbonization level of commercial building operations in the top five emitting megalopolises—Jing-Jin-Ji, Yangtze River Delta, Pearl River Delta, Yangtze River Middle Reach, and Cheng-Yu (see the definition in Appendix B)—considering socio-economic, technological evolution, and climate factors using the generalized Divisia index method (GDIM). Specifically, the GDIM decomposition technique is first used to identify the drivers of commercial building decarbonization. Based on the decomposition results, the decoupling status of decarbonization from economic growth is further evaluated. Finally, the historical decarbonization levels are evaluated from three emission scales, and the decarbonization efficiency is compared among megalopolises. In addition, deep decarbonization strategies are proposed to seek the best practice pathways by combining historical decarbonization levels with a review of current decarbonization efforts.

Regarding the most necessary contribution, this study is the first to estimate the historical decarbonization of commercial buildings from the megalopolises perspective to respond to the call for carbon peak and neutrality in China. For this purpose, this study examines the effects of socio-economic, technological evolution, and climate on the decarbonization and decoupling from the economic growth of commercial building operations and assesses and compares the historical decarbonization levels of five megalopolises at three levels: total, per floor space, and per capita.

The rest of this paper is structured as follows: Section 2 presents a literature review. Section 3 describes the methods and materials, covering the emission model, GDIM, the GDIM-based decoupling efforts index model, and the datasets. Section 4 provides the results of the drivers and the decoupling effect of operational carbon emissions. Section 5 includes three aspects: Section 5.1 shows the operational decarbonization estimation of commercial buildings. Section 5.2 compares the decarbonization efficiencies of the five megalopolises. Section 5.3 discusses the strategies of deep decarbonization toward net-zero emissions. Finally, Section 6 concludes the core findings and proposes future studies.

2. Literature review

In recent decades, megalopolises have gradually emerged worldwide and offer the best chance but also the greatest challenge for decarbonization [14, 15]. According to the latest statistics, the operational carbon emissions from commercial buildings in the five selected megalopolises have soared more than 3-fold since 2000 and as a whole contribute approximately half of the total energy consumption and operational carbon emissions in China's commercial buildings in 2018 [9] (see Fig. 1). Many studies on major Chinese emitting cities have highlighted the importance of megalopolises for decarbonizing commercial buildings [16], for instance, Jing-Jin-Ji [17, 18], Yangtze River Delta [19], Pearl River Delta [20], Guangdong-Hong Kong-Macao Greater Bay Area [21], and other important pilot cities [22, 23]. However, to our knowledge, existing studies only cover specific megalopolises or regions and lack comprehensive analysis and comparison. More importantly, most of these efforts have neglected the assessment of the historical operational decarbonization levels of commercial buildings.

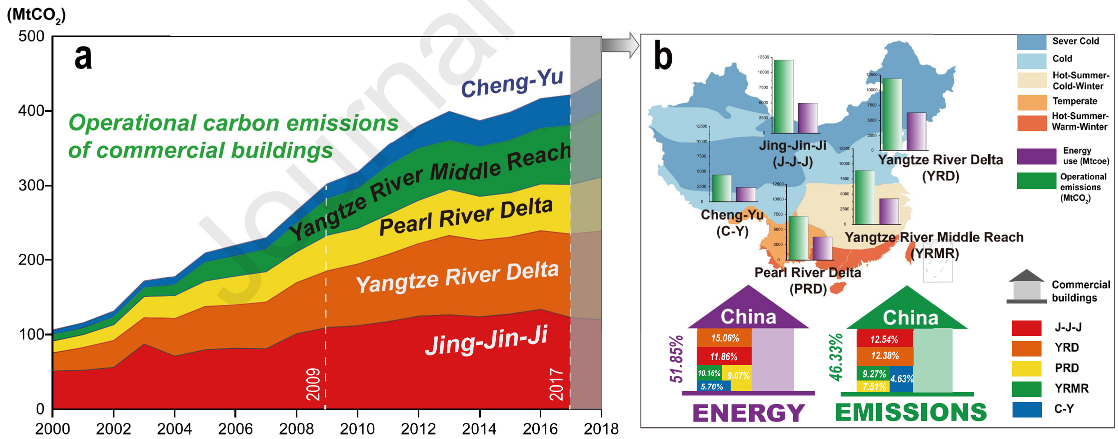

Fig. 1. (a) Operational carbon change of commercial buildings in five megalopolises (2000-2018) and (b) energy and emission levels from commercial buildings in 2018.

Regarding operational carbon emissions of buildings, index decomposition analysis (IDA), especially the log-mean decomposition index (LMDI) [24], is a key tool for measuring the driving forces of economic variables over time based on the Kaya identity [25]. Because of its advantages of simple operation and perfect decomposition, IDA has been widely used to analyze the influence of socioeconomic factors on operational carbon emissions and to further assess the decarbonization potential of the buildings sector [26, 27], including commercial buildings [28, 29], urban residential buildings [30], and rural residential buildings [31]. Moreover, with the continuous development of decomposition methods, increasing evidence suggests that the decomposition method based on Kaya identity is too dependent on the relationship between factors to output stable decomposition results [32]. This has led to better alternatives being proposed, such as the GDIM [33], decomposing structure decomposition [34] and Marshall-Edgeworth with structural effects decomposition [35].

Considering the existing research on carbon emissions released by commercial buildings described above, two gaps should be noted.

Regarding decarbonization assessment, although a large number of studies on decarbonization have been reported in the classical literature, they have mainly focused on the international or national level [36, 37]. For instance, Zhang et al. [38] compared the carbon mitigation of commercial buildings in China and the United States and concluded that the mitigation efficiency in China was 1.5 times that in the United States. Lin et al. [39] first used the LMDI to investigate the drivers of carbon change in the commercial buildings sector of China and provided corresponding policies to reduce emissions. Zhou et al. [40] and Tang et al. [41] further analyzed the low-carbon development trajectory of commercial buildings by the mid-century. Recently, Li et al. [2] reviewed the provincial decarbonization levels of commercial buildings in China and compared them with those at the national level. However, megalopolises, as major carriers of operational carbon released by commercial buildings, have not received the necessary attention to date.

Regarding the analytical approach to assessing building decarbonization, GDIM is the preferred decomposition method for assessing historical decarbonization. Compared with other conventional decomposition techniques, GDIM not only overcomes the inherent flaws in the traditional index decomposition analysis framework but also enables a multi-perspective analysis of the nonlinear interrelationships among potential driving forces [42, 43]. Namely, the GDIM can identify both absolute and relative indicators [44]. In addition, a large number of empirical analyses from the energy and emission sectors confirm the validity of this method [45, 46]. Therefore, GDIM has been used to reveal the main contributors and decarbonization processes in major emission sectors [47, 48], including industry [49], transportation [50], and electricity [51, 52]. However, to our knowledge, no studies on GDIM in the area of building operation emissions have yet been conducted.

Therefore, to fill these gaps, the historical evolution of carbon emissions of commercial buildings in five Chinese megalopolises is investigated using the GDIM decomposition method. The contributions cover two aspects.

- **This is the first time the operational carbon change of commercial buildings is reviewed via GDIM.** As mentioned earlier, the existing literature is mainly based on the classical index decomposition method, and analysis via GDIM in the building sector has not been reported. Therefore, this study first uses an advanced GDIM to identify the factors affecting operational carbon, then reviews the decoupling effect based on the decomposition results, and finally evaluates the historical decarbonization levels of commercial buildings.
- **The historical decarbonization levels of the top five megalopolises' commercial buildings are assessed across three scales for the first time.** Currently, only a few studies have conducted decarbonization assessments for commercial building operations, and none have emerged at the megalopolis level. This study allows for the vital role of China's megalopolises' buildings in carbon neutral actions. Operational decarbonization levels of commercial buildings are assessed on different scales: total decarbonization, decarbonization per floor space, and decarbonization per capita. Furthermore, the decarbonization efficiency of the five megalopolises is compared to explore the operational decarbonization potential of commercial buildings.

3. Methods and materials

The GDIM was adopted to explore the driving factors, decoupling effects, and mitigation of operational carbon emissions from commercial buildings in five megalopolises in China. The emission model for commercial building operations is described in Section 3.1. The GDIM approach used to determine the drivers of operational decarbonization of commercial buildings is presented in Section 3.2, and the GDIM-based decoupling effort index model is described in Section 3.3. Finally, data collection is presented in Section 3.4.

3.1. Operational carbon emission model

Ehrlich and Holden [53] developed an environmental impact model with population, affluence, and technology (IPAT) in 1971, which provides an important analytical framework for exploring the effects of environmental change [54]. The classical IPAT model is expressed as follows:

$$I = P \times A \times T \tag{1}$$

where *I* on the left-hand side of Eq. (1) represents the environmental impact caused by the influencing factors, and *P*, *A,* and *T* on the right-hand side of Eq. (1) represent population size, affluence level, and technology level, respectively. Correspondingly, the impact of carbon emissions can be described by the IPAT model as follows:

$$C = P \times \underbrace{\frac{G}{P}}_{A} \times \underbrace{\frac{C}{G}}_{T} \tag{2}$$

For the building sector, based on the emission characteristics and inherent properties of the commercial building sector, the emissions model [55] in Eq. (2) is redefined as:

$$C = P \times \underbrace{\frac{G}{P}}_{A} \times \underbrace{\frac{G_s}{G} \times \frac{F}{G_s} \times \frac{E}{F} \times \frac{C}{E}}_{T} \tag{3}$$

In previous studies, Eq. (3) was generally decomposed according to the index decomposition analysis method (e.g., LMDI [56]) as follows:

$$\Delta C|_{0\to T} = C|_T - C|_0 = \Delta C[P] + \Delta C\left[\frac{G}{P}\right] + \Delta C\left[\frac{G_s}{G}\right] + \Delta C\left[\frac{F}{G_s}\right] + \Delta C\left[\frac{E}{F}\right] + \Delta C\left[\frac{C}{E}\right] \tag{4}$$

where $\Delta C|_{0\rightarrow T}$ denotes the change in the total carbon emissions over the period $[0,T]$. The terms on the right-hand side (e.g., $\Delta C[P]$) of Eq. (4) represent the contribution level of population size to the operational carbon in buildings.

However, as stated in the literature review, the decomposition results (Eq. (4)) calculated using the conventional method have many drawbacks compared to the GDIM. Hence, a new emission model was proposed in this study to quantify the drivers of carbon emissions from commercial building operations based on the classical IPAT model, which is expressed as follows:

$$C = \underbrace{P \times \frac{C}{P}}_{P} = \underbrace{G \times \frac{C}{G}}_{A} = \underbrace{G_s \times \frac{C}{G_s} = F \times \frac{C}{F} = E \times \frac{C}{E}}_{T} \tag{5}$$

The GDIM was then applied to decompose the emission model proposed in this study.

3.2. Generalized Divisia index method (GDIM)

Following the theory and content of the GDIM, a commercial building operation emission model (Eq. (5)) proposed in this study can be rewritten as follows:

$$C = x_1 x_2 = x_3 x_4 = x_5 x_6 = x_7 x_8 = x_9 x_{10} \tag{6}$$

where x_1, x_3, x_5, x_7, x_9 are absolute factors and $x_2, x_4, x_6, x_8, x_{10}$ are relative factors. Then, the other four relative indicators can be further derived by

$$\begin{cases} x_{11} = \dfrac{x_6}{x_{10}} = \dfrac{C}{G_s} \Big/ \dfrac{C}{E} = \dfrac{E}{G_s} \\ x_{12} = \dfrac{x_6}{x_4} = \dfrac{C}{G} \Big/ \dfrac{C}{G_s} = \dfrac{Gs}{G} \\ x_{13} = \dfrac{x_2}{x_4} = \dfrac{C}{P} \Big/ \dfrac{C}{G} = \dfrac{G}{P} \\ x_{14} = \dfrac{x_8}{x_{10}} = \dfrac{C}{F} \Big/ \dfrac{C}{E} = \dfrac{E}{F} \end{cases} \tag{7}$$

Let the vector $\mathbf{x} = [x_1, x_2, x_3, \cdots, x_{14}]$, which represents the influencing factors that determine the carbon emissions of commercial building operations. The definitions and explanations of the influencing factors in vector $\mathbf{x}$ are summarized and tabulated in Table 1.

Table 1. The definition and explanation of driving factors in GDIM.

Driving factors	Definition	Explanation
x_1	P	Population size
x_2	$\frac{C}{P}$	Carbon emission per capita
x_3	G	GDP
x_4	$\frac{C}{G}$	Carbon emission per GDP
x_5	G_s	Service industry added value
x_6	$\frac{C}{G_s}$	Economic efficiency of emissions
x_7	F	Floor space
x_8	$\frac{C}{F}$	Carbon intensity
x_9	E	Energy consumption
x_{10}	$\frac{C}{E}$	Emission factor
x_{11}	$\frac{E}{G_s}$	Economic efficiency of energy
x_{12}	$\frac{Gs}{G}$	Industrial structure
x_{13}	$\frac{G}{P}$	GDP per capita
x_{14}	$\frac{E}{F}$	Energy intensity

Simultaneous Eqs. (6) and (7) are obtained as follows:

$$\begin{cases} C = x_5 x_6 \\ \theta_1 = x_5 x_6 - x_1 x_2 = 0 \\ \theta_2 = x_5 x_6 - x_3 x_4 = 0 \\ \theta_3 = x_5 x_6 - x_7 x_8 = 0 \\ \theta_4 = x_5 x_6 - x_9 x_{10} = 0 \\ \theta_5 = x_9 - x_5 \times x_{11} = 0 \\ \theta_6 = x_5 - x_3 \times x_{12} = 0 \\ \theta_7 = x_3 - x_1 \times x_{13} = 0 \\ \theta_8 = x_9 - x_7 \times x_{14} = 0 \end{cases} \tag{8}$$

Eq. (8) can be expressed in matrix form as:

$$\begin{cases} \mathbf{\Theta}(x) = 0 \\ C = f(\mathbf{x}) = f(x_1, x_2, \cdots, x_{14}) \end{cases} \tag{9}$$

According to [33], the change in carbon emissions from commercial buildings can be decomposed as

$$\Delta C[\mathbf{X}|\mathbf{\Theta}]^{\mathrm{T}} = \int_L \nabla C^{\mathrm{T}} \left(\mathbf{I} - \mathbf{\Theta}_x \mathbf{\Theta}_x^{+}\right) \mathrm{d}\mathbf{X} \tag{10}$$

where L is the time interval, $\mathbf{I}$ is the identity matrix, $\nabla C = (x_5, x_6, 0,0,0,0,0,0,0,0,0,0,0,0)^{\mathrm{T}}$ is the gradient of the function $f(\mathbf{x})$ with respect to the influence factor, $\mathbf{\Theta}_x$ is the Jacobi matrix of the matrix function $\boldsymbol{\Theta}(x)$ and satisfies $(\boldsymbol{\Theta}_x)_{ij} = \frac{\partial \theta_j}{\partial x_i}$. In this study, $\boldsymbol{\Theta}_x$ reflects the marginal impact of different drivers on carbon emissions from commercial building operations and is defined as follows:

$$\boldsymbol{\Theta}_x = \begin{pmatrix} -x_2 & -x_1 & 0 & 0 & x_6 & x_5 & 0 & 0 & 0 & 0 & 0 & 0 & 0 & 0 \\ 0 & 0 & -x_4 & -x_3 & x_6 & x_5 & 0 & 0 & 0 & 0 & 0 & 0 & 0 & 0 \\ 0 & 0 & 0 & 0 & x_6 & x_5 & -x_8 & -x_7 & 0 & 0 & 0 & 0 & 0 & 0 \\ 0 & 0 & 0 & 0 & x_6 & x_5 & 0 & 0 & -x_{10} & -x_9 & 0 & 0 & 0 & 0 \\ 0 & 0 & 0 & 0 & -x_{11} & 0 & 0 & 0 & 1 & 0 & -x_5 & 0 & 0 & 0 \\ 0 & 0 & -x_{12} & 0 & 1 & 0 & 0 & 0 & 0 & 0 & 0 & -x_3 & 0 & 0 \\ -x_{13} & 0 & 1 & 0 & 0 & 0 & 0 & 0 & 0 & 0 & 0 & 0 & -x_1 & 0 \\ 0 & 0 & 0 & 0 & 0 & 0 & -x_{14} & 0 & 1 & 0 & 0 & 0 & 0 & -x_7 \end{pmatrix}_{8\times 14}^{T} \tag{11}$$

In addition, superscript $+$ in Eq. (10) represents the generalized inverse matrix operator, and $\boldsymbol{\Theta}_x^{+} = (\boldsymbol{\Theta}_x^{\mathrm{T}}\boldsymbol{\Theta}_x)^{-1}\boldsymbol{\Theta}_x^{\mathrm{T}}$ is satisfied when the Jacobian matrix column is full-rank. At this time, Eq. (10) can be further transformed into

$$\Delta C[\mathbf{X}|\boldsymbol{\Theta}]^{\mathrm{T}} = \int_L \nabla C^T \left(\mathbf{I} - \boldsymbol{\Theta}_x(\boldsymbol{\Theta}_x^{+}\boldsymbol{\Theta}_x)^{-1}\boldsymbol{\Theta}_x^{\mathrm{T}}\right)\mathrm{d}\mathbf{X} \tag{12}$$

The Simpson integral rule was used to integrate Eq. (12), and the change in commercial building emissions can be perfectly decomposed into the sum of the contributions of the 14 factors:

$$\Delta C|_{0\to T} = C|_T - C|_0 = \sum_{i=1}^{14} \Delta C[x_i] \tag{13}$$

Furthermore, the decarbonization ($\Delta DC|_{0\to T}$) of commercial building operations during period ΔT can be calculated using the emission drivers with negative contributions from 0 to *T*, which is defined as follows [57]:

$$\Delta DC|_{0\to T} = \sum \left|\Delta C\left[x_j\right]\right| \tag{14}$$

where $\Delta C\left[x_j\right] = \left\{\Delta C[x_i], i = 1,2,\cdots,14 \mid \Delta C[x_i] \le 0\right\}$. Accordingly, the decarbonization per floor space ($\Delta DF|_{0\to T}$) and decarbonization per capita ($\Delta DP|_{0\to T}$) can also be defined according to Eq. (14), as follows:

$$\begin{cases} \Delta DF|_{0\to T} = \dfrac{\Delta DC|_{0\to T}}{F} \\ \Delta DP|_{0\to T} = \dfrac{\Delta DC|_{0\to T}}{P} \end{cases} \tag{15}$$

3.3. The GDIM-based decoupling efforts index model

According to the decomposition results obtained through the GDIM, the change in operational carbon due to the change in GDP (ΔG) and GDP per capita change ($\Delta \frac{G}{P}$) can be regarded as economic growth effects [58, 59]. In general, decarbonization efforts are the sum of the factors (excluding economic growth effects) that lead to the reduction of operational carbon emissions from commercial buildings, and represent all efforts that directly or indirectly lead to operational decarbonization. Thus, the operational decarbonization effort from the base year to year T is characterized as [60]

$$\Delta D|_{0\to T} = \Delta C|_{0\to T} - (\Delta G + \Delta G_S) = \Delta C|_{0\to T} - (\Delta x_3 + \Delta x_{13}) \tag{16}$$

Furthermore, the decarbonization effort offset by the economic growth effect was used to assess the coupling effect between economic growth and the decarbonization of commercial buildings [61]. As illustrated in Eq. (17):

$$\varphi|_{0\to T} = \frac{\Delta D|_{0\to T}}{\Delta x_3 + \Delta x_{13}} \tag{17}$$

where $\varphi|_{0\to T}$ denotes the degree of decoupling of commercial buildings decarbonized during period [0, T]. The definitions of the different decoupling states are summarized in Table 2.

Table 2. The definition of decoupling state.

Decoupling state	$\Delta x_3 + \Delta x_{13}$	$\Delta D|_{0\to T}$	$\varphi|_{0\to T}$
Strong decoupling	> 0	< 0	$\varphi|_{0\to T} < -1$
Weak decoupling	> 0	< 0	$-1 < \varphi|_{0\to T} < 0$
Expansive negative decoupling	> 0	> 0	$\varphi|_{0\to T} > 0$
Strong negative decoupling	< 0	> 0	$\varphi|_{0\to T} < -1$
Weak negative decoupling	< 0	> 0	$-1 < \varphi|_{0\to T} < 0$
Recessive decoupling	< 0	< 0	$\varphi|_{0\to T} > 0$

Evidently, a decoupling indicator can be determined for each decomposition factor based on the additivity and comparability of the decomposition factors. To reveal the influencing factors driving the change in decoupling status, the decoupling indexes related to energy intensity and emission intensity are attributed to technical effects in this study, while the remaining decoupling indexes that do not directly reflect technological progress are identified as non-technical effects [62, 63]. Thus, the decoupling index for the decarbonization of commercial building operations can be decomposed as

$$\varphi|_{0\to T}=\frac{\Delta x_1+\Delta x_5+\Delta x_7+\Delta x_9+\Delta x_{12}}{\Delta x_3+\Delta x_{13}}+\frac{\Delta x_2+\Delta x_4+\Delta x_6+\Delta x_8+\Delta x_{10}+\Delta x_{11}+\Delta x_{14}}{\Delta x_3+\Delta x_{13}}$$
$$=\underbrace{\frac{\Delta x_1+\Delta x_5+\Delta x_7+\Delta x_9+\Delta x_{12}}{\Delta x_3+\Delta x_{13}}}_{Non-technical\ effect}+\underbrace{\frac{\Delta x_2+\Delta x_3+\Delta x_2+\Delta x_3+\Delta x_2+\Delta x_3+\Delta x_2}{\Delta x_3+\Delta x_{13}}}_{Technical\ effect} \quad (18)$$

For convenience, Eq. (18) is rewritten as follows:

$$\varphi|_{0\to T}=\underbrace{\varphi_{x_1}+\varphi_{x_5}+\varphi_{x_7}+\varphi_{x_9}+\varphi_{x_{12}}}_{Non-technical\ effect}+\underbrace{\varphi_{x_2}++\varphi_{x_4}+\varphi_{x_6}+\varphi_{x_8}+\varphi_{x_{10}}+\varphi_{x_{11}}+\varphi_{x_{14}}}_{Technical\ effect}$$
$$=\varphi_{Non-tech}+\varphi_{Tech} \quad (19)$$

where φ_{x_i} denotes the relative contribution level of the *i*th influencing factor to the overall decoupling effort index $\varphi|_{0\to T}$, and $\varphi_{Non-tech}$ and φ_{Tech} reflect the influence of technical and non-technical effects, respectively, on the decoupling of carbon emissions from commercial building operations.

3.4. Datasets

In this study, historical data from five megalopolises in China from 2000 to 2018 were selected as the research sample for use in a commercial building emission model. Fig. 2 and Tables C1-C5 (see Appendix C) show the descriptive statistics of all raw data, including population, GDP, service industry added value, building stock, and energy and emissions of commercial buildings. Building-related data were sourced from the IBED database (www.researchgate.net/project/International-Building-Emission-Dataset-IBED), which is a multi-regional dataset that mainly serves the building sector. Indicators related to population and economy were collected from http://data.stats.gov.cn/english/.

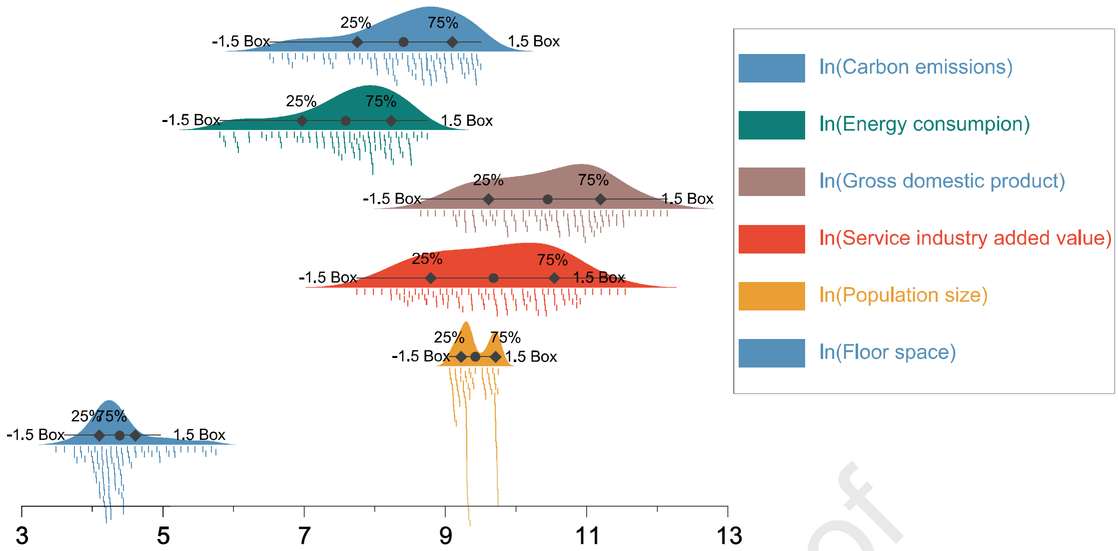

Fig. 2. Descriptive statistics of historical data for five megalopolises in China (2000–2018). Notes: the short vertical lines under the density plot indicate the sample, and the dots and diamonds in the density plot indicate the sample mean and 25th (75th) percentile, respectively.

4. Results

4.1. Drivers of operational decarbonization in commercial buildings

Based on the emission model established in Eq. (6), the change in carbon emissions from building operations was decomposed by the GDIM into the contributions of 14 driving factors, including five absolute drivers and nine relative drivers. The heat maps in Fig. 3 present the changes in the operational carbon emissions of commercial buildings and the decomposition results for the five megalopolises in China from 2000 to 2018.

Fig. 3 shows the total effect of the drivers. Operational carbon of commercial buildings in megalopolises continued to rise from 106.5 $MtCO_2$ in 2000 to 444.9 $MtCO_2$ in 2018, with an average annual growth rate of 17.7%. The most significant rise occurred in the Yangtze River Delta ($\Delta C_{\mathrm{Y-R-D}}|_{2000\rightarrow2018} =$ 94.7 $MtCO_2$), followed by the Yangtze River Middle Reach ($\Delta C_{\mathrm{Y-R-M-R}}|_{2000\rightarrow2018} =$ 80.1 $MtCO_2$). The carbon emissions of all megalopolises had a brief peak around 2014, and most megalopolises started to rebound strongly after peaking. Notably, in Jing-Jin-Ji, the operational carbon emissions of commercial buildings maintained a steady decline after peaking at 134.2 $MtCO_2$ in 2016. In addition, the effect of climate on changes in operational carbon is striking. Following the building climate zones provided by standard GB 50352-2019 (see Fig. 1 b) [64], the operational carbon emissions in hot summer/cold winter zones (Yangtze River Middle Reach: 55.6%, Cheng-Yu: 30.9%, Yangtze River Delta: 21.7%) had substantially higher average increase rates than those in hot summer/warm winter zones (Pearl River Delta: 19.6%) and cold zones (Jing-Jin-Ji: 7.5%).

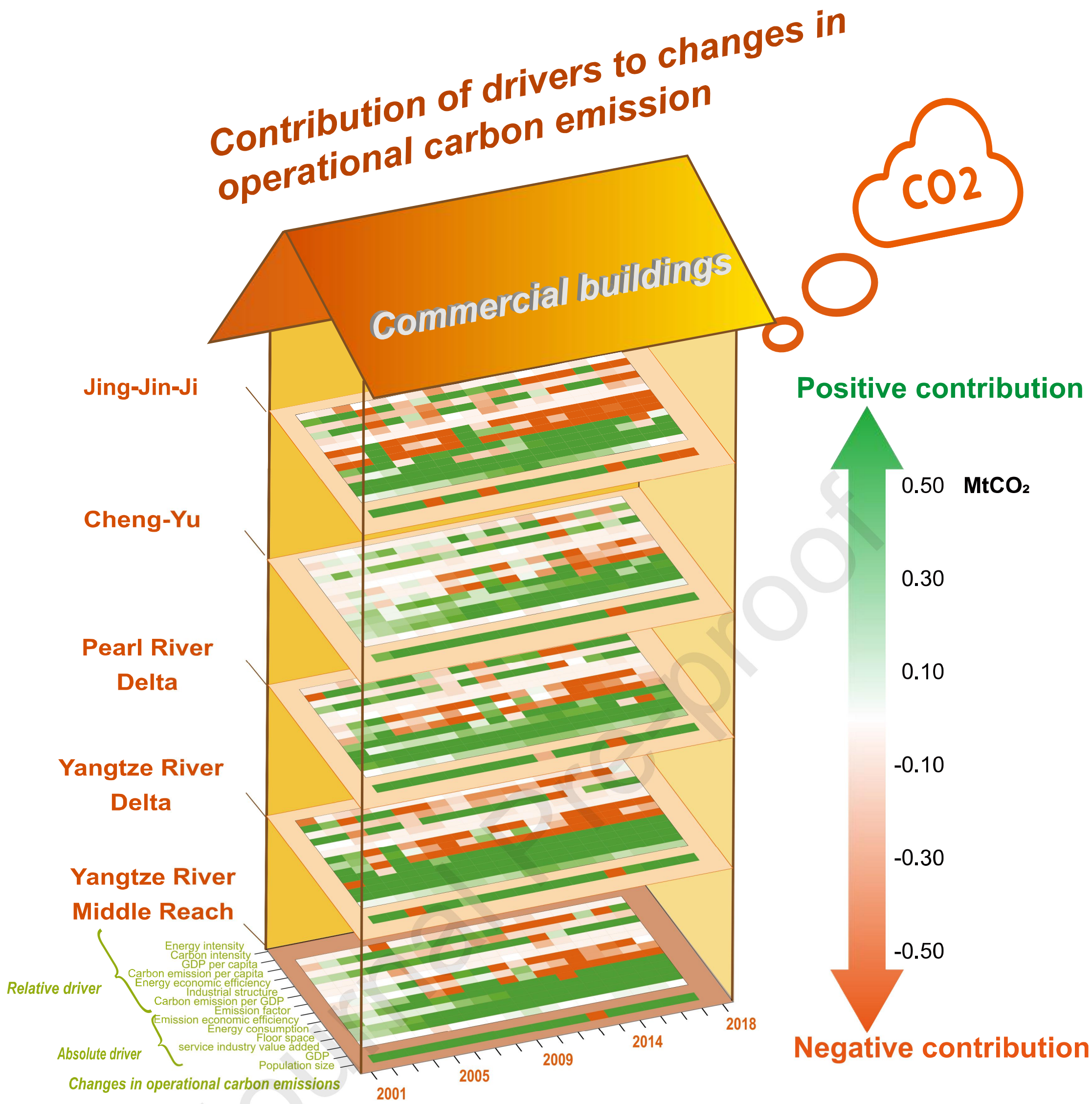

Fig. 3. Contribution of drivers to change in operational carbon emissions in five Chinese megalopolises.

As shown in the heat map in Fig. 3, the impact of drivers on the operational carbon emissions of commercial buildings from different megalopolises is similar. For the drivers that contribute to operational carbon emissions, the two largest contributors were the service industry added value (42.2%) and GDP (36.5%), both of which contributed consistently to the operational carbon of commercial buildings, especially for commercial buildings in Jing-Jin-Ji (59.4% and 68.9%). Another key factor driving carbon emissions was energy consumption (23.8%), which contributed to increases of 28.0% (Jing-Jin-Ji), 23.0% (Cheng-Yu), 22.7% (Pearl River Delta), 22.9% (Yangtze River Delta), and 22.4% (Yangtze River Middle Reach) in the five megalopolises. In addition, floor space (14.1%) also had a small positive impact on the carbon emissions of commercial buildings.

For drivers that contribute to decarbonization, the economic efficiency of emissions (-20.4%) and carbon emissions per GDP (-15.1%) played a critical role in driving the decarbonization of commercial building operations. In addition, the emission factor (-3.5%) was also an important driver of the decarbonization of commercial buildings, especially after 2014 (before 2014: -1.2%, after 2014: -4.2%). In contrast, the contribution of carbon emissions per capita and carbon intensity to decarbonization was not stable. For instance, carbon intensity had a positive contribution in Jing-Jin-Ji and Yangtze River Delta, whereas it was negative in the rest of the megalopolises. Additionally, the effect of carbon emission per capita on carbon emissions varied greatly from one period to another and shows large fluctuations. The remaining drivers had insignificant effects on carbon emissions and were, therefore, ignored.

Overall, the above decomposition results portray the major drivers driving the operational decarbonization of commercial buildings in megalopolises in China and respond to the first question raised in Section 1.

4.2. Decoupling effect of operational carbon in commercial buildings

After identifying the drivers of commercial building decarbonization, based on the decomposition results from the GDIM, the decoupling effort index model was used to investigate the decoupling effect of operational carbon of commercial buildings, and the results are illustrated in Fig. 4. For ease of analysis and comparison, the study period was divided into four phases: 2000–2005, 2006–2009, 2010–2014, and 2015–2018. Since the 21st century, China's service economy has always maintained rapid development, resulting in the economic growth of the five megalopolises showing an increasing trend. Therefore, the decoupling results (see the map in Fig. 4 a) only cover three decoupling states: expansion negative decoupling, weak decoupling, and strong decoupling.

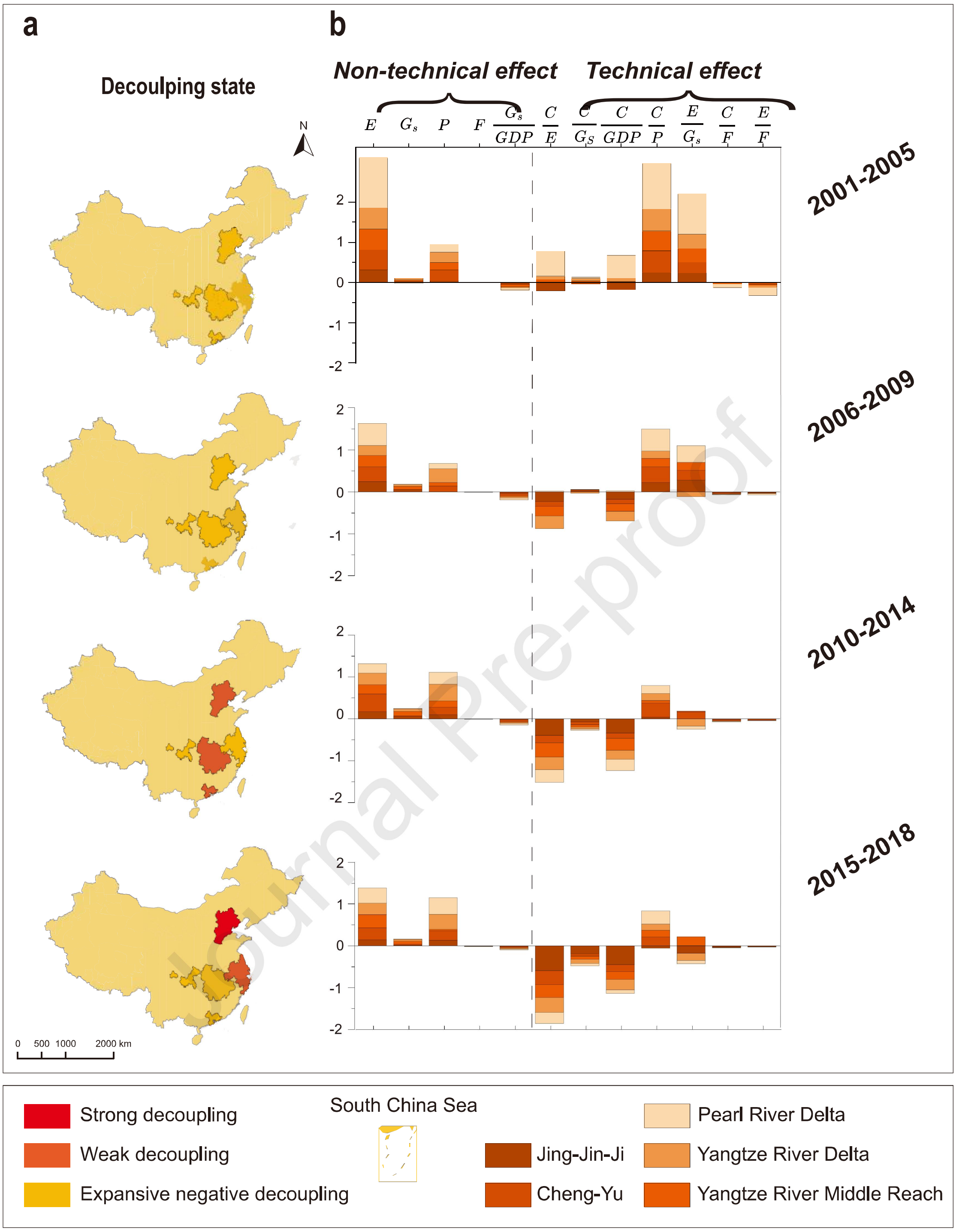

Fig. 4. (a) The decoupling state of operational carbon in commercial buildings and (b) the drivers of changes in the decoupling state.

Fig. 4 a presents the evolution of the decoupling of operational carbon emissions from 2000 to 2018, and the results show that the average decoupling indexes of the five megalopolises from 2000 to 2018 were: 1.96 (2000–2005), 0.63 (2006–2009), 0.02 (2010–2014), and -0.08 (2015–2018). This indicates that the decoupling efforts of carbon emissions from commercial building operations have been increasing, from the initial expansion negative decoupling to weak decoupling. Specifically, before 2009, the decoupling effort index of the decarbonization of commercial buildings in the five megalopolises was greater than zero, showing an expansion negative decoupling state, indicating that the carbon emissions of commercial building operations and economic growth effects in these regions have not been decoupling, that is, the decarbonization efforts during this period could not offset the increase in carbon emissions driven by economic effects. Since 2009, except for the Cheng-Yu region, which still maintains the negative decoupling state, the rest of the megalopolises started to show a state of less than zero or even less than -1, indicating that these regions have entered a deep decoupling state, and the decarbonization effect caused by the constraints has been gradually offset or even exceed the driving effect brought by the economic growth effect. In other words, the operational carbon in these regions decreased with the growth of economic effects, including GDP and the service industry added value. To be more specific, from 2009 to 2014, operational carbon in the Jing-Jin-Ji region$\left(\varphi_{\mathrm{J-J-J}}|_{2009\to2014} = -0.48\right)$, the Pearl River Delta ($\varphi_{\mathrm{P-R-D}}|_{2009\to2014} = -0.15$) and the Yangtze River Middle Reach ($\varphi_{\mathrm{Y-R-M-R}}|_{2009\to2014} = -0.04$) were the first to show a weak decoupling state. During 2015–2018, the Yangtze River Delta ($\varphi_{\mathrm{Y-R-D}}|_{2015\to2018} = -0.08$) also entered a weak decoupling state, and the Pearl River Delta ($\varphi_{\mathrm{P-R-D}}|_{2015\to2018} = 0.18$) and Yangtze River Delta ($\varphi_{\mathrm{Y-R-D}}|_{2015\to2018} = 0.57$) returned to the expansion negative decoupling state, and the Jing-Jin-Ji region entered a strong decoupling state.

Fig. 4b further provides the drivers of change in the decoupling of carbon emissions from commercial buildings. For all megalopolises, the decoupling efforts index of technology effects decreased continuously throughout the study period ($\varphi_{Tech}|_{2000\to2005} = 0.84, \varphi_{Tech}|_{2006\to2009} = 0.12, \varphi_{Tech}|_{2010\to2014} = -0.35, \varphi_{Tech}|_{2015\to2018} = -0.43$) , while non-technology effects changed insignificantly and always led to an increase in the decoupling efforts index ($\varphi_{Non-Tech}|_{2000\to2005} = 0.78, \varphi_{Non-Tech}|_{2006\to2009} = 0.46, \varphi_{Non-Tech}|_{2010\to2014} = 0.50, \varphi_{Non-Tech}|_{2015\to2018} = 0.52$), indicating that changes in decoupling of operational carbon in megalopolises were mainly driven by technological effects. From the decoupling efforts index of the drivers, emission factor and carbon emission per GDP were key technical factors that led to the decoupling of operational carbon emissions from economic growth effects. Additionally, although some of the remaining technical factors (such as carbon emission per capita and economic efficiency of energy) had a dampening effect on the decoupling of operational carbon emissions, this effect gradually diminished or even reversed. Energy consumption and population size determined the non-technical effects.

Overall, the above results present the change in decoupling effect of operational carbon from economic growth in megalopolises and the reason behind this transformation, answering the second question posed in Section 1.

5. Discussion

The deep decarbonization of megalopolises is an important prerequisite for China to accomplish its ambitious blueprint for net-zero emissions. Therefore, to close the gap between the current carbon mitigation progress of commercial buildings and the existing targets, megalopolises should make more prominent contributions. In this section, the historical decarbonization levels from 2000 to 2018 are discussed. Section 5.1 traces the dynamic evolution of the operational decarbonization of commercial buildings in three aspects (including total decarbonization, decarbonization per floor space, and decarbonization per capita), and Section 5.2 compares the decarbonization efficiency of megalopolises at different stages. Finally, Section 5.3 reviews the energy efficiency and emission reduction policies of commercial buildings in China's megalopolises, and the corresponding policy insights are stated based on historical decarbonization levels.

5.1. Operational decarbonization assessment of commercial buildings

As described in Section 3.2, based on the GDIM decomposition results, the historical decarbonization level of commercial buildings can be evaluated using Eqs. (13–15), and the results are presented in Fig. 6. The size of the bubbles on the map reflects the total cumulative decarbonization in the Chinese megalopolises' commercial buildings. From 2000 to 2018, the five megalopolises have decarbonized a total of 233.1 $MtCO_2$, which is equivalent to 4.4% of the total operational carbon emissions; the megalopolis with the highest level of total decarbonization was the Jing-Jin-Ji region with 102.0 $MtCO_2$ (equivalent to the total emissions of the five megalopolises in 2000 or the sum of the cumulative decarbonization in Cheng-Yu, Yangtze River Delta, and Yangtze River Middle Reach), followed by the Yangtze River Delta (55.4 $MtCO_2$), the Yangtze River Middle Reach (29.9 $MtCO_2$), and the Pearl River Delta (29.5 $MtCO_2$), whereas the megalopolis with the lowest total decarbonization was the Cheng-Yu region, with 16.3 $MtCO_2$ (less than 1/6 of Jing-Jin-Ji's decarbonization).

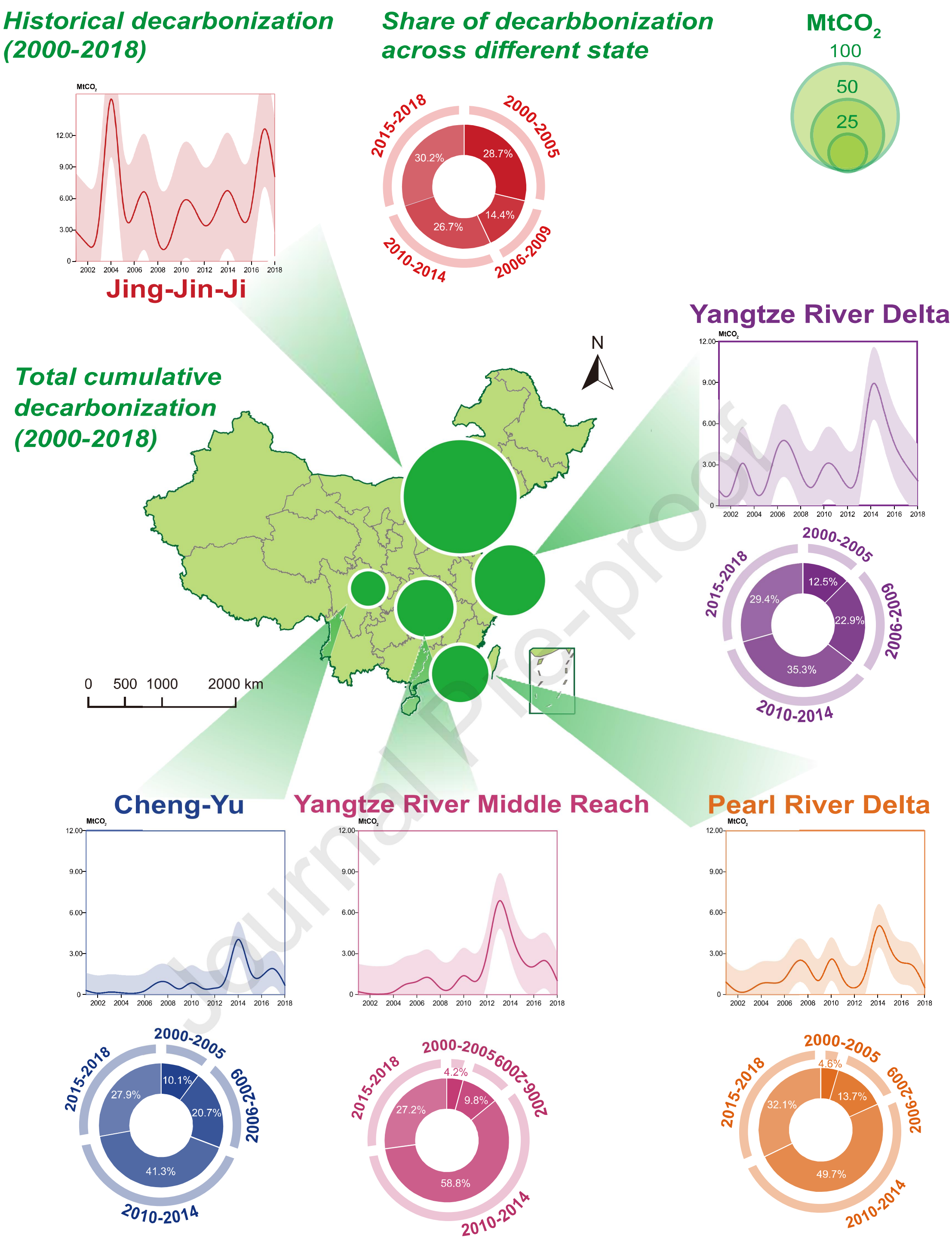

Fig. 5. Operational decarbonization change of commercial buildings in megalopolises and share of decarbonization at different stages (2000–2018). Note: the bubbles on the map indicate the total cumulative decarbonization from 2000 to 2018; the error bands in the line graph indicate one standard deviation.

From the perspective of the specific historical trajectory of decarbonization, during the entire study period, the decarbonization trajectory of commercial building operations in China's megalopolises generally showed an upward trend. Specifically, as the top two megalopolises with the largest emissions, the decarbonization in the Jing-Jin-Ji and the Yangtze River Delta regions was always significantly higher than that of the other three megalopolises during the same period and fluctuated more significantly, with annual average decarbonization of 5.7 $MtCO_2$/yr and 3.1 $MtCO_2$/yr respectively, peaking in 2004 (22.7 $MtCO_2$) and 2014 (10.8 $MtCO_2$), respectively. In contrast, the changes in the decarbonization of commercial buildings located in the remaining three megalopolises were relatively stable and very similar. From 2000 to 2012, the total decarbonization in these regions was relatively low, and the total decarbonization between 2012 and 2018 showed an M-shape with all peaks around 2014. The total annual average decarbonization of Yangtze River Middle Reach, Pearl River Delta, and Cheng-Yu was 1.7 $MtCO_2$/yr, 1.6 $MtCO_2$/yr, and 0.9 $MtCO_2$/yr, respectively. With respect to the change in stage decarbonization, from 2000 to 2018, the share of total decarbonization in the five megalopolises across the four stages was 15.8%, 18.6%, 32.6%, and 33.0%, respectively, indicating that the operational decarbonization process of commercial buildings was gradually accelerating.

Fig. 6 further depicts the change of decarbonization per floor space and per capita in China's megalopolises. From 2001 to 2018, the average annual decarbonization per floor space of the five megalopolises is ranked as follows: Jing-Jin-Ji (7.8 $kgCO_2/m^2$/yr) > Pearl River Delta (2.3 $kgCO_2/m^2$/yr) > Yangtze River Delta (2.0 $kgCO_2/m^2$/yr) > Yangtze River Middle-Reach (1.5 $kgCO_2/m^2$/yr) > Cheng-Yu (1.3 $kgCO_2/m^2$/yr). Further, the ranking of average annual decarbonization per capita is: Jing-Jin-Ji (55.6 $kgCO_2$ per capita/yr) > Yangtze River Delta (19.5 $kgCO_2$ per capita/yr) > Pearl River Delta (15.3 $kgCO_2$ per capita/yr) > Yangtze River Middle Reach (9.8 $kgCO_2$ per capita/yr) > Cheng-Yu (8.1 $kgCO_2$ per capita/yr). In general, the megalopolis with the highest level of decarbonization from the three scales was Jing-Jin-Ji (especially in terms of per floor space and per capita, which both exceed the combined total of the remaining megalopolises), while the lowest was Cheng-Yu. Although there is a huge gap between the total amount of decarbonization in Cheng-Yu and the other megalopolises, the decarbonization per floor space and decarbonization per capita in Cheng-Yu are close to other megalopolises, especially the Yangtze

River Middle Reach. In addition, the decarbonization per floor space and decarbonization per capita in the Pearl River Delta and in the Yangtze River Delta are very similar, but the total amount of decarbonization in the Yangtze River Delta is almost twice that of the Pearl River Delta.

Overall, the above discussion estimates the operational decarbonization of commercial buildings in five megalopolises at three scales over the last decade, tentatively answering the third question posed in Section 1.

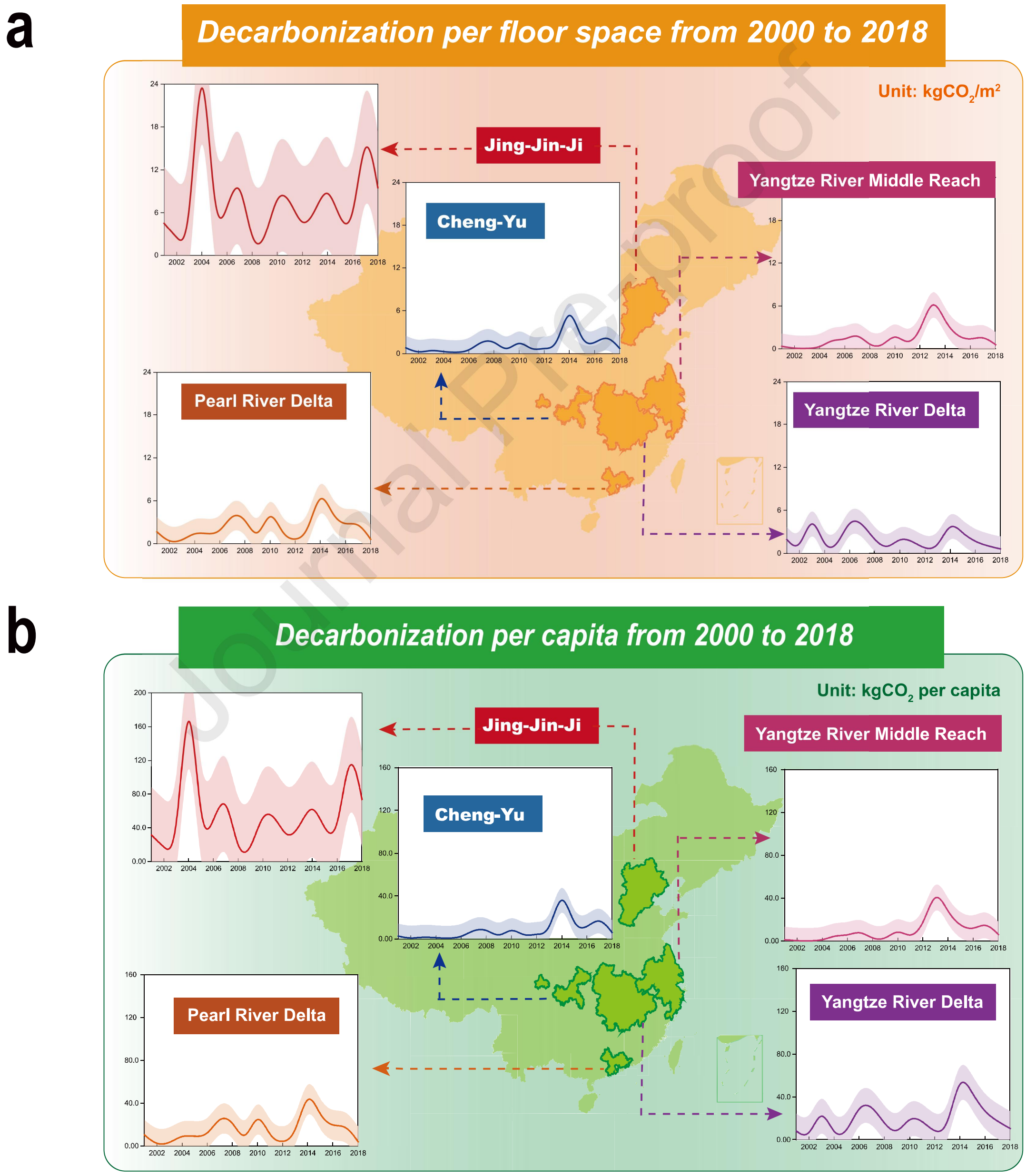

Fig. 6. (a) Operational decarbonization per floor space and (b) per capita of commercial buildings in the five Chinese megalopolises.

5.2. Comparison of decarbonization efficiency of the five megalopolises

Although Section 5.1 assesses the operational decarbonization level of commercial buildings in China from three emission scales, this assessment framework, which relies only on absolute indicators, is incomplete. To gain insight into the decarbonization potential and thus allocate future emission shares for each megalopolis [65]. In this section, decarbonization efficiency is introduced into the assessment framework of this study, which is defined as the ratio of total decarbonization to carbon emissions. Similarly, the intensity-based decarbonization efficiency can also be calculated. Fig. 7 a–c shows the decarbonization efficiency of China's megalopolises at three emission scales: total amount, per capita, and per floor space, respectively. Meanwhile, the decarbonization efficiency is very close at different scales, which is caused by insignificant changes in population size and floor space within each period. Therefore, the following discussion takes the total amount of decarbonization as an example to compare the decarbonization efficiency between megalopolises.

As shown in Fig. 7, the decarbonization efficiency in Jing-Jin-Ji and Yangtze River Delta was consistently higher than that of the other megalopolises between 2000 and 2018. From 2000 to 2005, the commercial building operations in Jing-Jin-Ji reduced carbon emissions by 29.2 $MtCO_2$, accounting for 28.7% of the total decarbonization, which is equivalent to 8.4% of the operational carbon emissions of Jing-Jin-Ji during the same period. The decarbonization efficiency during this time period was the highest of all megalopolises during the entire study period. After 2005, the decarbonization efficiency in Jing-Jin-Ji steadily increased (3.9%, 4.5%, and 6.1%), whereas the opposite was true for the Yangtze River Delta (4.8%, 4.1%, 3.7%). For commercial building operations in Cheng-Yu, Pearl River Delta, and Yangtze River Middle Reach, decarbonization efficiency increased steadily during 2000–2014 and then decreased. Although total decarbonization in the Yangtze River Middle Reach and Pearl River Delta were very close and had similar trends, the decarbonization efficiency in the Pearl River Delta was higher than that in the Yangtze River Middle Reach (except for the period 2006–2018). In addition, although the total decarbonization of Cheng-Yu was much smaller than that of the Pearl River Delta region, the decarbonization efficiencies of both were very similar from 2000 to 2018. The overall decarbonization efficiency of commercial buildings in the five megalopolises from to 2000– 2018 was Jing-Jin-Ji (5.6%) >

Yangtze River Delta (4.0%) > Cheng-Yu (3.8%) > Yangtze River Middle Reach (3.5%) = Pearl River Delta (3.5%).

In summary, the above discussion compares the decarbonization efficiency of different megalopolises, further answering the third question posed in Section 1.

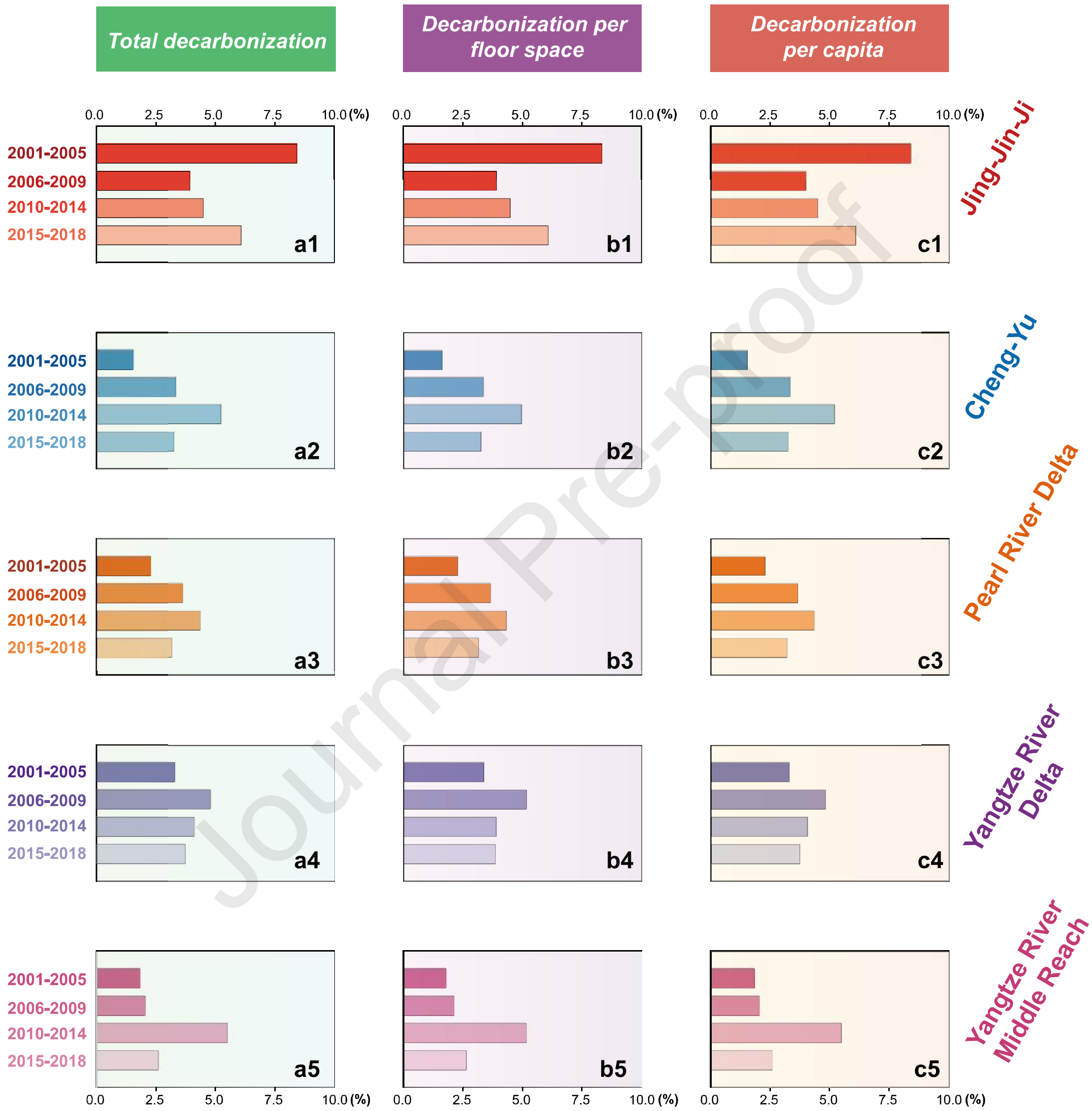

Fig. 7. Operational decarbonization efficiency of commercial buildings at different scales: (a1-a5) total, (b1-b5) per floor space, and (c1-c5) per capita.

5.3. Deep decarbonization strategies toward net-zero emissions

Sections 5.1 and 5.2 report the operational decarbonization levels of commercial buildings in megalopolises. Although the results show that the pace of decarbonization in megalopolises is accelerating, the overall decarbonization efficiency is still relatively low (ranging from 3.5% to 5.6%). The deep decarbonization of building operations is closely related to improvements in energy conservation levels. Since 1980, the Chinese government has proposed a series of energy conservation standards to improve the energy efficiency of commercial building operations and thus reduce operational carbon emissions, as well as the concepts of ultralow, near-zero, and zero energy buildings. Following these policies, the regions in which megalopolises are located have proposed corresponding policies that consider climatic conditions and specific situations. Fig. 8 outlines the roadmap of decarbonization strategies for commercial buildings over the last few decades.

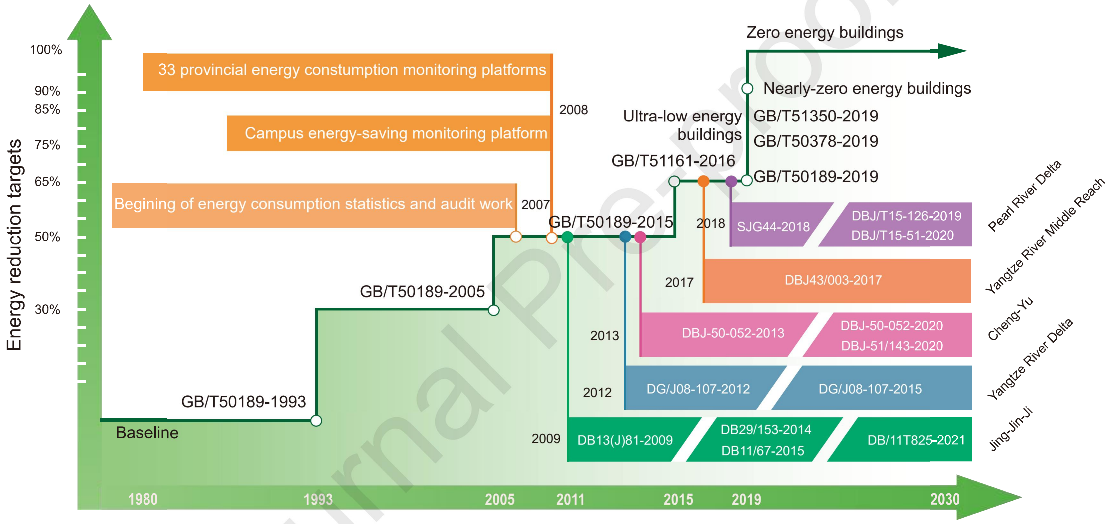

Fig. 8. The roadmap of decarbonization strategies for the commercial buildings in China.

Combining the proposed findings and existing energy conversion policies, future decarbonization strategies for China’s megalopolises can be implemented in two ways.

From the perspective of megalopolises, the agglomeration effect of megalopolises should be maximized, thereby promoting the development of emerging industries and industrial structure upgrading [66]. The Chinese government has already launched three batches of low-carbon pilot cities in seven provinces and 80 cities since 2010 and accomplished initial achievements [67, 68], and more attention needs to be paid simultaneously to resource allocation and the spatial layout of megalopolises to combat environmental threats caused by rapid urbanization (e.g., urban heat island effect [69]). In addition, unified and more advanced energy efficiency standards and evaluation systems for buildings can help improve the energy efficiency of the construction industry within megalopolises; for example, the Jing-Jin-Ji region jointly promulgated the *Design Standard Of Green Buildings* in 2021 [70]. In addition, some advanced experiences from abroad are worth learning from, such as the vertical greening system implemented in Singapore [71, 72] and the net-zero energy building goal proposed in California [73].

From the perspective of building operations, end-use electrification should be promoted, and the proportion of renewable energy in building operations should be significantly increased [74, 75], especially for megalopolises located in cold northern regions (e.g., the Jing-Jin-Ji region). Meanwhile, strengthening the supervision and management of energy consumption monitoring and auditing in commercial buildings is recommended (e.g., Shanghai [76] and Shenzhen [77]), where the provision of large amounts of online monitoring data will effectively constrain the energy intensity of the end-use equipment [78, 79]. In addition to these, the government should guide the development of low-carbon technologies by improving the fiscal incentive system or using economic instruments (e.g., carbon taxes [80] and carbon markets [81]) and digital financial inclusion [82].

Overall, the policy recommendations for the deep decarbonization of commercial buildings address the third question posed in Section 1.

6. Conclusion

This study investigated the progress of decarbonization of commercial building operations in China's megalopolises using the GDIM. First, the GDIM was applied to identify the driving forces of operational carbon emissions from 2000 to 2018. Based on the decomposition results, the decoupling state of operational carbon emissions was characterized by the decoupling efforts index. Second, the study assessed the historical decarbonization level on the three emission scales. Third, decarbonization efficiency was investigated to determine the potential for deep decarbonization. Finally, policies to decarbonize commercial building operations in megalopolises were reviewed to identify potential pathways to net-zero emissions. The findings are summarized as follows:

6.1. Main findings

- **Operational carbon emissions from commercial buildings continued to rise at an annual level of 17.7%, with economic growth effects and energy use being the key drivers contributing to the rise.** Carbon emissions from commercial building operations in five megalopolises continued to rise from 106.5 $MtCO_2$ in 2000 to 444.9 $MtCO_2$ in 2018. In addition, the economic growth effect [service industry added value (42.2%) and GDP (36.5%)] was the largest contributor promoting operational carbon emissions (especially for commercial buildings in the Jing-Jin-Ji region), followed by energy consumption (23.8%). In contrast, the economic efficiency of emissions (-20.4%), carbon emissions per GDP (-15.1%), and emission factor (-3.5%) were the key drivers for decarbonizing building operations.
- **Since 2009, operational carbon emissions were decoupled from economic growth effects in most megalopolises (except the Cheng-Yu).** From 2000 to 2009, there was a clear coupling effect between operational carbon emissions and economic growth in commercial buildings. After 2009, operational carbon in Jing-Jin-Ji, Pearl River Delta, and Yangtze River Middle Reach decoupled from economic growth effects and displayed a weak decoupling in 2010–2014. During 2015–2018, the Yangtze River Delta also displayed a weak decoupling state, and Jing-Jin-Ji presented a strong decoupling state. Following the decoupling effort index of drivers,

technical effects were key contributors to the decoupling of operational carbon from economic growth, whereas non-technical effects had always prevented it.

- **The operational decarbonization of commercial buildings of megalopolises was gradually accelerating, with cumulative decarbonization of 233.1 $MtCO_2$ from 2000 to 2018, with the highest decarbonization level in the Jing-Jin-Ji region (5.7 $MtCO_2$/yr, 7.8 $kgCO_2/m^2$/yr, 55.6 $kgCO_2$ per capita per yr).** This study assessed and compared the decarbonization level and efficiency of commercial building operations in megalopolises on three scales. From 2000 to 2018, the total decarbonization of the five megalopolises of Jing-Jin-Ji, Yangtze River Delta, Yangtze River Middle Reach, Pearl River Delta, and Cheng-Yu was 5.7, 3.1, 1.7, 1.6, and 0.9 $MtCO_2$/yr, which corresponds to 5.6%, 4.0%, 3.5%, 3.5%, and 3.8% of their respective total carbon emissions. Moreover, the decarbonization per floor space for these regions was 7.8, 2.0, 1.5, 2.3 and 1.3 $kgCO_2/m^2$/yr, and the decarbonization per capita for these regions was 55.6, 19.5, 9.8, 15.3 and 8.1 $kgCO_2$ per capita per yr respectively.

6.2. Future direction

To further deepen the theme of decarbonization and accelerate the process of moving commercial buildings toward net-zero emissions, several other issues deserve future investigation. Because commercial buildings rely heavily on fossil energy for their energy consumption and serve end-use activities such as space heating and water heating, the influence of end-use behavior and energy structure on carbon emissions from commercial buildings should be further investigated in detail in future studies. Although the decarbonization assessment in this work provides a baseline level of historical emissions for commercial buildings, the projected decarbonization potential of commercial buildings is still unclear. Therefore, an assessment framework for evaluating future decarbonization of building operations should be developed to clarify the roadmap for deep decarbonization. In addition, the remaining budget and allocation of carbon emissions from commercial buildings at the megalopolis level should also be addressed as a priority in future studies, which would help control the total amount of carbon emissions from commercial building operations to ease the pressure on China to achieve its carbon peak by 2030.

Acknowledgment

This study was supported by the Graduate Research and Innovation Foundation of Chongqing, China (CYS22071), the National Planning Office of Philosophy and Social Science Foundation of China (21CJY030), the Beijing Natural Science Foundation (8224085), the China Postdoctoral Science Foundation (2020M680020), and the Shuimu Tsinghua Scholar Program of Tsinghua University (2019SM139).

Appendix

Please find the Appendix A-C in the supplementary materials (e-component) of this submission.

References

[1] Probst B, Touboul S, Glachant M, Dechezleprêtre A. Global trends in the invention and diffusion of climate change mitigation technologies. Nature Energy 2021;6:1077-1086.

[2] Li K, Ma M, Xiang X, Feng W, Ma Z, Cai W, et al. Carbon reduction in commercial building operations: A provincial retrospection in China. Applied Energy 2022;306:118098.

[3] Xiang X, Ma X, Ma Z, Ma M. Operational Carbon Change in Commercial Buildings under the Carbon Neutral Goal: A LASSO–WOA Approach. Buildings 2022;12:54.

[4] Qiu Y, Kahn ME. Better sustainability assessment of green buildings with high-frequency data. Nature Sustainability 2018;1:642-649.

[5] Azimi S, O'Brien W. Fit-for-purpose: Measuring occupancy to support commercial building operations: A review. Building and Environment 2022;212:108767.

[6] Yu W, Shi J, Fang Y, Xiang A, Li X, Hu C, et al. Exploration of urbanization characteristics and their effect on the urban thermal environment in Chengdu, China. Building and Environment 2022;219:109150.

[7] Ruan T, Rim D. Indoor air pollution in office buildings in mega-cities: Effects of filtration efficiency and outdoor air ventilation rates. Sustainable Cities and Society 2019;49:101609.

[8] Dong L, Longwu L, Zhenbo W, Liangkan C, Faming Z. Exploration of coupling effects in the Economy–Society–Environment system in urban areas: Case study of the Yangtze River Delta Urban Agglomeration. Ecological Indicators 2021;128:107858.

[9] Ma M, Ma X, Cai W, Cai W. Low carbon roadmap of residential building sector in China: Historical mitigation and prospective peak. Applied Energy 2020;273:115247.

[10] Ye Z, Cheng K, Hsu S-C, Wei H-H, Cheung CM. Identifying critical building-oriented features in city-block-level building energy consumption: A data-driven machine learning approach. Applied Energy 2021;301:117453.

[11] Ji W, Zhao K, Zhao B. The trend of natural ventilation potential in 74 Chinese cities from 2014 to 2019: Impact of air pollution and climate change. Building and Environment 2022;218:109146.

[12] Zhou Y, Zhao H, Mao S, Zhang G, Jin Y, Luo Y, et al. Studies on urban park cooling effects and their driving factors in China: Considering 276 cities under different climate zones. Building and Environment 2022;222:109441.

[13] Zhang J, Yu Z, Cheng Y, Chen C, Wan Y, Zhao B, et al. Evaluating the disparities in urban green space provision in communities with diverse built environments: The case of a rapidly urbanizing Chinese city. Building and Environment 2020;183:107170.

[14] Lu H, de Jong M, Song Y, Zhao M. The multi-level governance of formulating regional brand identities: Evidence from three Mega City Regions in China. Cities 2020;100:102668.

[15] Taveres-Cachat E, Grynning S, Thomsen J, Selkowitz S. Responsive building envelope concepts in zero emission neighborhoods and smart cities - A roadmap to implementation. Building and Environment 2019;149:446-457.

[16] Chen C, Bi L. Study on spatio-temporal changes and driving factors of carbon emissions at the building operation stage- A case study of China. Building and Environment 2022;219:109147.

[17] Wang Y, Hu D, Yu C, Di Y, Wang S, Liu M. Appraising regional anthropogenic heat flux using high spatial resolution NTL and POI data: A case study in the Beijing-Tianjin-Hebei region, China. Environmental Pollution 2022;292:118359.

[18] Liu H, Mauzerall DL. Costs of clean heating in China: Evidence from rural households in the Beijing-Tianjin-Hebei region. Energy Economics 2020;90:104844.

[19] Yu C, Hu D, Wang S, Chen S, Wang Y. Estimation of anthropogenic heat flux and its coupling analysis with urban building characteristics – A case study of typical cities in the Yangtze River Delta, China. Science of The Total Environment 2021;774:145805.

[20] Lv Y, Peng H, He M, Huang Y, Wang J. Definition of typical commercial building for South China's Pearl River Delta: Local data statistics and model development. Energy and Buildings 2019;190:119-131.

[21] Geng J, Wang J, Huang J, Zhou D, Bai J, Wang J, et al. Quantification of the carbon emission of urban residential buildings: The case of the Greater Bay Area cities in China. Environmental Impact Assessment Review 2022;95:106775.

[22] Cai M, Shi Y, Ren C. Developing a high-resolution emission inventory tool for low-carbon city management using hybrid method – A pilot test in high-density Hong Kong. Energy and Buildings 2020;226:110376.

[23] Pan W, Du J. Impacts of urban morphological characteristics on nocturnal outdoor lighting environment in cities: An empirical investigation in Shenzhen. Building and Environment 2021;192:107587.

[24] Sun Y, Hao Q, Cui C, Shan Y, Zhao W, Wang D, et al. Emission accounting and drivers in East African countries. Applied Energy 2022;312:118805.

[25] Lu Y, Cui P, Li D. Carbon emissions and policies in China's building and construction industry: Evidence from 1994 to 2012. Building and Environment 2016;95:94-103.

[26] Chen X, Shuai C, Wu Y, Zhang Y. Analysis on the carbon emission peaks of China's industrial, building, transport, and agricultural sectors. Science of The Total Environment 2020;709:135768.

[27] Lu Y, Cui P, Li D. Which activities contribute most to building energy consumption in China? A hybrid LMDI decomposition analysis from year 2007 to 2015. Energy and Buildings 2018;165:259-269.

[28] Zhong X, Hu M, Deetman S, Rodrigues JFD, Lin H-X, Tukker A, et al. The evolution and future perspectives of energy intensity in the global building sector 1971–2060. Journal of Cleaner Production 2021;305:127098.

[29] He J, Yue Q, Li Y, Zhao F, Wang H. Driving force analysis of carbon emissions in China’s building industry: 2000–2015. Sustainable Cities and Society 2020;60:102268.

[30] Lin B, Liu H. CO2 mitigation potential in China's building construction industry: A comparison of energy performance. Building and Environment 2015;94:239-251.

[31] Zhang M, Song Y, Li P, Li H. Study on affecting factors of residential energy consumption in urban and rural Jiangsu. Renewable and Sustainable Energy Reviews 2016;53:330-337.

[32] Shao S, Liu J, Geng Y, Miao Z, Yang Y. Uncovering driving factors of carbon emissions from China's mining sector. Applied Energy 2016;166:220-238.

[33] Vaninsky A. Factorial decomposition of CO2 emissions: A generalized Divisia index approach. Energy Economics 2014;45:389-400.

[34] Boratyński J. Decomposing structural decomposition: The role of changes in individual industry shares. Energy Economics 2021;103:105587.

[35] Roux N, Kastner T, Erb K-H, Haberl H. Does agricultural trade reduce pressure on land ecosystems? Decomposing drivers of the embodied human appropriation of net primary production. Ecological Economics 2021;181:106915.

[36] Yang X, Hu M, Zhang C, Steubing B. Key strategies for decarbonizing the residential building stock: Results from a spatiotemporal model for Leiden, the Netherlands. Resources, Conservation and Recycling 2022;184:106388.

[37] Ohene E, Chan APC, Darko A. Prioritizing barriers and developing mitigation strategies toward net-zero carbon building sector. Building and Environment 2022;223:109437.

[38] Zhang S, Ma M, Li K, Ma Z, Feng W, Cai W. Historical carbon abatement in the commercial building operation: China versus the US. Energy Economics 2022;105:105712.

[39] Lin B, Liu H. CO2 emissions of China's commercial and residential buildings: Evidence and reduction policy. Building and Environment 2015;92:418-431.

[40] Zhou N, Khanna N, Feng W, Ke J, Levine M. Scenarios of energy efficiency and CO2 emissions reduction potential in the buildings sector in China to year 2050. Nature Energy 2018;3:978-984.

[41] Tang B-J, Guo Y-Y, Yu B, Harvey LDD. Pathways for decarbonizing China's building sector under global warming thresholds. Applied Energy 2021;298:117213.

[42] Yu Y, Zhou X, Zhu W, Shi Q. Socioeconomic driving factors of PM2.5 emission in Jing-Jin-Ji region, China: a generalized Divisia index approach. Environmental Science and Pollution Research 2021;28:15995-16013.

[43] Yan R, Xiang X, Cai W, Ma M. Decarbonizing residential buildings in the developing world: Historical cases from China. Science of The Total Environment 2022;847:157679.

[44] Pan Y, Dong F. Dynamic evolution and driving factors of new energy development: Fresh evidence from China. Technological Forecasting and Social Change 2022;176:121475.

[45] Wang J, Jiang Q, Dong X, Dong K. Decoupling and decomposition analysis of investments and CO2 emissions in information and communication technology sector. Applied Energy 2021;302:117618.

[46] Miao Z, Liu S, Chen X. Driving factors and spatio-temporal features underlying industrial SO2 emissions in "2+26" in North China and extended cities. Chinese Journal of Population, Resources and Environment 2020;18:296-318.

[47] Li B, Han S, Wang Y, Wang Y, Li J, Wang Y. Feasibility assessment of the carbon emissions peak in China's construction industry: Factor decomposition and peak forecast. Science of The Total Environment 2020;706:135716.

[48] Zhang X, Geng Y, Shao S, Wilson J, Song X, You W. China's non-fossil energy development and its 2030 CO2 reduction targets: The role of urbanization. Applied Energy 2020;261:114353.

[49] Wen H-x, Chen Z, Yang Q, Liu J-y, Nie P-y. Driving forces and mitigating strategies of CO2 emissions in China: A decomposition analysis based on 38 industrial sub-sectors. Energy 2022;245:123262.

[50] Wang Y, Zhou Y, Zhu L, Zhang F, Zhang Y. Influencing Factors and Decoupling Elasticity of China's Transportation Carbon Emissions. Energies 2018;11:1157.

[51] Fang D, Hao P, Yu Q, Wang J. The impacts of electricity consumption in China's key economic regions. Applied Energy 2020;267:115078.

[52] Yan Q, Wang Y, Baležentis T, Streimikiene D. Analysis of China's regional thermal electricity generation and CO2 emissions: Decomposition based on the generalized Divisia index. Science of The Total Environment 2019;682:737-755.

[53] Ehrlich Paul R, Holdren John P. Impact of Population Growth. Science 1971;171:1212-1217.

[54] York R, Rosa EA, Dietz T. STIRPAT, IPAT and ImPACT: analytic tools for unpacking the driving forces of environmental impacts. Ecological Economics 2003;46:351-365.

[55] Zhang S, Ma M, Xiang X, Cai W, Feng W, Ma Z, et al. Potential to decarbonize the commercial building operation of the top two emitters by 2060. Resources, Conservation and Recycling 2022;185:106481.

[56] Xiang X, Ma X, Ma Z, Ma M, Cai W. Python-LMDI: A Tool for Index Decomposition Analysis of Building Carbon Emissions. Buildings 2022;12:83.

[57] Xiang X, Ma M, Ma X, Chen L, Cai W, Feng W, et al. Historical decarbonization of global commercial building operations in the 21st century. Applied Energy 2022;401:119401.

[58] Wang Y, Su X, Qi L, Shang P, Xu Y. Feasibility of peaking carbon emissions of the power sector in China's eight regions: decomposition, decoupling, and prediction analysis. Environmental Science and Pollution Research 2019;26:29212-29233.

[59] Shuai C, Zhao B, Chen X, Liu J, Zheng C, Qu S, et al. Quantifying the impacts of COVID-19 on Sustainable Development Goals using machine learning models. Fundamental Research 2022.

[60] Diakoulaki D, Mandaraka M. Decomposition analysis for assessing the progress in decoupling industrial growth from CO2 emissions in the EU manufacturing sector. Energy Economics 2007;29:636-664.

[61] Chen X, Shuai C, Wu Y, Zhang Y. Understanding the sustainable consumption of energy resources in global industrial sector: Evidences from 114 countries. Environmental Impact Assessment Review 2021;90:106609.

[62] Yu B, Fang D. Decoupling economic growth from energy-related PM2.5 emissions in China: A GDIM-based indicator decomposition. Ecological Indicators 2021;127:107795.

[63] Liu J, Yang Q, Ou S, Liu J. Factor decomposition and the decoupling effect of carbon emissions in China's manufacturing high-emission subsectors. Energy 2022;248:123568.

[64] Wang Z, Xu J, Wang Y, Wang LW, Wang RZ. Annual energy simulation for the air conditioning of Fuxing high speed trains. Applied Thermal Engineering 2021;188:116591.

[65] Gan L, Ren H, Cai W, Wu K, Liu Y, Liu Y. Allocation of carbon emission quotas for China's provincial public buildings based on principles of equity and efficiency. Building and Environment 2022;216:108994.

[66] Chen X, Zhao B, Shuai C, Qu S, Xu M. Global spread of water scarcity risk through trade. Resources, Conservation and Recycling 2022;187:106643.

[67] Zhang H, Sun X, Bi C, Ahmad M, Wang J. Can sustainable development policy reduce carbon emissions? Empirical evidence from resource-based cities in China. Science of The Total Environment 2022;838:156341.

[68] Tang P, Zeng H, Fu S. Local government responses to catalyse sustainable development: Learning from low-carbon pilot programme in China. Science of The Total Environment 2019;689:1054-1065.

[69] Zhang L, Yang X, Fan Y, Zhang J. Utilizing the theory of planned behavior to predict willingness to pay for urban heat island effect mitigation. Building and Environment 2021;204:108136.

[70] Beijing_Municipal_Commission_of_Housing_and_Urban-Rural_Development. Design Standard Of Green Buildings, http://scjgj.beijing.gov.cn/zwxx/gs/dfbzgg/202104/t20210408_2349427.html; 2021 [accessed May 20]. in Chinese.

[71] Tan PY, Wang J, Sia A. Perspectives on five decades of the urban greening of Singapore. Cities 2013;32:24-32.

[72] Coma J, Pérez G, de Gracia A, Burés S, Urrestarazu M, Cabeza LF. Vertical greenery systems for energy savings in buildings: A comparative study between green walls and green facades. Building and Environment 2017;111:228-237.

[73] Stadler M, Kloess M, Groissböck M, Cardoso G, Sharma R, Bozchalui MC, et al. Electric storage in California's commercial buildings. Applied Energy 2013;104:711-722.

[74] Johnson RC, Royapoor M, Mayfield M. A multi-zone, fast solving, rapidly reconfigurable building and electrified heating system model for generation of control dependent heat pump power demand profiles. Applied Energy 2021;304:117663.

[75] Li R, Satchwell AJ, Finn D, Christensen TH, Kummert M, Le Dréau J, et al. Ten questions concerning energy flexibility in buildings. Building and Environment 2022;223:109461.

[76] Wang L, Zheng D. Integrated analysis of energy, indoor environment, and occupant satisfaction in green buildings using real-time monitoring data and on-site investigation. Building and Environment 2020;182:107014.

[77] Ma J-J, Du G, Zhang Z-K, Wang P-X, Xie B-C. Life cycle analysis of energy consumption and CO2 emissions from a typical large office building in Tianjin, China. Building and Environment 2017;117:36-48.

[78] Zhang L, Wen J, Li Y, Chen J, Ye Y, Fu Y, et al. A review of machine learning in building load prediction. Applied Energy 2021;285:116452.

[79] Yin H, Zhai X, Ning Y, Li Z, Ma Z, Wang X, et al. Online monitoring of PM2.5 and CO2 in residential buildings under different ventilation modes in Xi'an city. Building and Environment 2022;207:108453.

[80] Zhang Y, Qi L, Lin X, Pan H, Sharp B. Synergistic effect of carbon ETS and carbon tax under China's peak emission target: A dynamic CGE analysis. Science of The Total Environment 2022;825:154076.

[81] Ren X, Li Y, yan C, Wen F, Lu Z. The interrelationship between the carbon market and the green bonds market: Evidence from wavelet quantile-on-quantile method. Technological Forecasting and Social Change 2022;179:121611.

[82] Wang X, Wang X, Ren X, Wen F. Can digital financial inclusion affect CO2 emissions of China at the prefecture level? Evidence from a spatial econometric approach. Energy Economics 2022;109:105966.

Highlights

- GDIM was used to investigate drivers, decoupling, and mitigation of operational carbon changes.
- The effects of economic development and energy use are key to increasing operational carbon.
- Operational carbon emissions decoupled from economic effects in most megalopolises since 2009.
- Decarbonization level in five megalopolises was 233.1 Mt, with a decarbonization efficiency of 4.4%.
- Deep decarbonization strategies for commercial building operations in megalopolises were reviewed.

Declaration of interests

☒ The authors declare that they have no known competing financial interests or personal relationships that could have appeared to influence the work reported in this paper.

☐ The authors declare the following financial interests/personal relationships which may be considered as potential competing interests: